Architecture, Not Scale: Circuit Localization in Large Language Models

Anonymous Authors[1]

Abstract

Mechanistic interpretability assumes that circuit analysis becomes harder as models scale. We challenge this assumption by showing that the attention architecture matters more than parameter count. Studying three circuit types across Pythia and Qwen2.5, we find that grouped query attention produces circuits that are far more concentrated and mechanistically stable than standard multi-head attention at comparable scales. The same concentration pattern holds across indirect object identification, induction heads and factual recall. Within a single architecture family (Qwen2.5), factual recall circuits undergo a discrete phase transition above a critical scale, collapsing to a single bottleneck rather than degrading gradually. These findings suggest that some architectural choices make large models more tractable to study and that interpretability difficulty is not a fixed consequence of model size.

1. Introduction

Mechanistic interpretability aims to reverse-engineer neural networks into understandable components such as circuits, features and representations that explain specific model behaviors (Olah et al., 2020; Elhage et al., 2021). The core premise is that models encode computations in identifiable structures that can be located, ablated and understood. This has proven productive on small models (Olsson et al., 2022; Wang et al., 2022; Meng et al., 2022) but a practical concern remains: does mechanistic interpretability stay feasible as models scale to billions of parameters?

The standard assumption is that it does not. Larger models are expected to develop more redundant representations, distribute computation across more components and resist the surgical ablations that make small-model circuits legible (Lindsey et al., 2025; Elhage et al., 2022). This belief shapes how the field allocates effort, prioritising small tractable models and developing automated tools designed to cope with future scale (Conmy et al., 2023). The assumption has rarely been tested directly under controlled conditions. Prior work studying interpretability at scale has not controlled for architecture as an independent variable (Lieberum et al., 2023).

We isolate one key variable, the attention mechanism. We compare Pythia (Biderman et al., 2023), which uses standard Multi-Head Attention (MHA) throughout, against Qwen2.5 (Yang et al., 2024), which uses Grouped Query Attention (GQA) throughout. We test three circuit types (indirect object identification, induction heads and factual recall) across six model sizes from 160M to 7B parameters using TransformerLens (Nanda & Bloom, 2022).

Architecture predicts circuit geometry more reliably than scale. GQA models produce circuits that concentrate into one or two heads across all three tasks. MHA models produce circuits that spread across tens to hundreds of heads. The difference follows from the structural constraints GQA imposes on value-space computation. Ablating one KV head disrupts all query heads sharing it, creating a bottleneck with no analogue in MHA.

GQA circuits are also mechanistically stable. The same head dominates regardless of task difficulty or input distribution. MHA circuits shift substantially between easy and hard input conditions, with the top contributing heads changing across regimes. This stability asymmetry matters for safety monitoring. Consistent circuit behavior across inputs is a prerequisite for reliable oversight (Ganguli et al., 2022).

2. Related Work

Induction heads. Olsson et al. (2022) identified induction heads as a key mechanism for in-context learning across transformer architectures. These heads implement a pattern-completion operation: given a repeated sequence $[A][B] \dots [A]$, they attend back to the first A and copy the subsequent B. We measure how induction circuit geometry changes with scale and architecture.

Indirect object identification. Wang et al. (2022) identified the IOI circuit in GPT-2 small using activation patch-

[1]Anonymous Institution, Anonymous City, Anonymous Region, Anonymous Country. Correspondence to: Anonymous Author <anon.email@domain.com>.

Preliminary work. Under review by the International Conference on Machine Learning (ICML). Do not distribute.

ing, characterising name mover heads, backup name mover heads and inhibition heads. IOI and induction heads are distinct circuit types. IOI requires semantic name tracking across sentence structure and routing of the object name to the prediction position. Induction heads implement a mechanical copy operation that does not require semantic understanding (McDougall et al., 2024). We use IOI as our primary evaluation task and extend it across two architecture families.

Factual recall. Meng et al. (2022) located factual associations in mid-to-late MLP layers using causal tracing. Geva et al. (2023) characterised the role of attention heads in routing subject information to the final token position. Earlier work by Geva et al. (2021) established that feed-forward layers function as key-value memories.

Scaling and interpretability. Conmy et al. (2023) proposed Automatic Circuit DisCovery (ACDC), which uses iterative activation patching to identify the minimal computational subgraph implementing a target behaviour. Lieberum et al. (2023) tested whether circuit analysis scales to Chinchilla-scale models and found mixed evidence. Standard techniques transferred to the 70B model but semantic understanding of the identified components remained partial. Lindsey et al. (2025) find that circuits in larger language models are denser and harder to isolate. We ask whether architectural choices can produce large models tractable by existing methods.

Features and representations. Elhage et al. (2022) showed that networks store more features than dimensions through superposition. Templeton (2024) showed sparse autoencoders decompose these into interpretable features at scale. Marks & Tegmark (2023) found emergent linear structure in truth representations. Hernandez et al. (2023) showed relation decoding is linear in transformer representations.

3. Background

Induction heads. An induction head attends from a repeated token $[A]$ back to its previous occurrence and copies the subsequent token as its prediction. This enables in-context learning: the model completes novel patterns seen earlier in context (Olsson et al., 2022). Induction heads typically operate as a two-head system. A previous-token head shifts attention back one position and an induction head uses this signal to attend to the token that followed the prior occurrence.

Indirect Object Identification. The IOI task requires identifying the recipient in sentences such as "After Mary and John went to the store, John gave a mango to ___", where the correct answer is Mary. This differs fundamentally from induction: the model must track two names, determine their semantic roles and route the correct name to the prediction position. Wang et al. (2022) decomposed this circuit into name mover heads, backup name mover heads and inhibition heads. We measure circuit geometry using logit difference $\text{logit}(\text{IO}) - \text{logit}(\text{S})$ at the final token, where IO is the recipient and S is the giver.

Factual recall. Factual recall refers to completing subject-relation-object associations stored in model weights, for example completing "The capital of France is" with "Paris". The circuit involves subject token processing and attention heads that route subject information to the final token position (Geva et al., 2023). Prior work using causal tracing (Meng et al., 2022) located factual associations in mid-to-late MLP layers of MHA models.

Grouped Query Attention. Standard MHA (Cordonnier et al., 2020) gives each attention head independent query, key and value matrices. With h heads, head i computes:

$$\text{Attn}_i = \text{softmax}\left(\frac{Q_i K_i^\top}{\sqrt{d_{\text{head}}}}\right) V_i \tag{1}$$

GQA shares key and value matrices across groups of query heads, with $n_{\text{kv}} < h$ KV heads (Ainslie et al., 2023):

$$\text{Attn}_i = \text{softmax}\left(\frac{Q_i K_{\lfloor i/r \rfloor}^\top}{\sqrt{d_{\text{head}}}}\right) V_{\lfloor i/r \rfloor}, \quad r = h/n_{\text{kv}} \tag{2}$$

This reduces KV cache size by r and concentrates value-space computation into n_{kv} shared subspaces. A single KV head mediates the output of all r query heads assigned to it.

4. Methodology

4.1. Models

We study two architecture families. Pythia comprises Pythia-160M (12 layers, 12 heads), Pythia-1.4B (24 layers, 16 heads) and Pythia-6.9B (32 layers, 32 heads). Qwen2.5 comprises Qwen2.5-0.5B (24 layers, 14 Q-heads, 2 KV-heads), Qwen2.5-1.5B (28 layers, 12 Q-heads, 2 KV-heads) and Qwen2.5-7B (28 layers, 28 Q-heads, 4 KV-heads).

4.2. Tasks

We study three circuit types that are well-established in the mechanistic interpretability literature and each probe a distinct kind of computation.

Indirect Object Identification (IOI) is our primary task. IOI has a known circuit structure from prior work (Wang et al., 2022), making it the strongest test of whether architecture affects circuit geometry on a well-characterised semantic task.

We use the fahamu/ioi dataset (Fahamu, 2023), containing 26M IOI sentences. We sample 500 sentences per model and filter to ensure both names tokenise to exactly one token, preventing multi-token ambiguity in the logit difference metric. We score each (layer, head) pair using 20 sentences by measuring the logit difference drop when that head is ablated. Ablation curves run over the full 500-sentence set.

Induction heads serve as a robustness check on a task with no semantic content. If the same concentration pattern appears on synthetic repeated-token sequences as on IOI, it is unlikely to be specific to name-tracking. We construct 200 random repeated-token sequences of the form $[\text{prefix}][A][B][\text{suffix}][A]$ and measure ICL loss: the cross-entropy of predicting $[B]$ at the final position. For each (layer, head) pair we measure mean attention weight at the AB offset position and run greedy ablation curves.

Factual recall uses a curated set of 493 subject-completion facts spanning ten domains. We build a custom set rather than using existing benchmarks because TriviaQA and similar datasets contain multi-token answers and multi-hop chains that complicate single-head ablation analysis. All facts in our set have single-token answers and known subject-relation-object structure. Pythia prompts use natural completion format. Qwen2.5 prompts use a QA format that reliably elicits factual answers from instruction-aware models. We apply top-3 filtering for both families. We run two conditions: a per-model condition using facts each model answers correctly and a shared condition using the intersection of facts known by all models in a family, which controls for fact difficulty when comparing across scales.

4.3. Metrics

We report two main metrics. Top head score is the logit or accuracy drop from ablating the single most important head. Higher values indicate a more dominant single head. Heads-to-80% counts the greedy ablations needed to cause 80% task damage. Lower values indicate a more concentrated circuit.

5. Results

5.1. GQA Concentrates IOI Circuits into One Head

Table 1 reports IOI results across both families. All six models solve the task with positive baseline logit difference, confirming task competence before circuit analysis.

All three Qwen2.5 models require one ablation for 80% damage while Pythia requires two to five. Qwen2.5 top head scores are four to eight times higher than Pythia at comparable scales. Pythia top head layers shift progressively deeper with scale (L8, L12, L16). Figure 1 shows head contribution score heatmaps at matched scales and Figure 2 shows how logit diff damage accumulates as heads are ablated in greedy order.

Table 2 shows that ablating the single top head alone causes damage comparable to the full greedy sequence, ruling out greedy ordering as the source of the heads-to-80% result.

Table 2. Single-head necessity check for Qwen2.5 IOI circuits. Logit Diff (post-ablation) is the logit difference after ablating the top-scoring head alone. Drop (%) is the percentage reduction from the baseline logit difference.

Model	Logit Diff (post-ablation)	Drop (%)
Qwen2.5-0.5B	-0.146	137.5
Qwen2.5-1.5B	-1.030	175.3
Qwen2.5-7B	$+0.082$	89.6

For Qwen2.5-0.5B and 1.5B, ablating the single top head causes logit difference to flip sign. The model actively predicts the wrong name after ablation. For Qwen2.5-7B, ablating the top head causes 89.6% damage. Ablating a randomly chosen mid-layer head as a negative control causes no damage and in several cases improves logit difference. This confirms the effect is circuit-specific and not a general consequence of value zeroing.

Qwen2.5-0.5B concentrates at layer 23 while Qwen2.5-1.5B and 7B concentrate at layer 0. This shift mirrors the phase transition in factual recall and points to a consistent architectural threshold above which GQA circuits reorganise to the earliest attention layer.

5.2. Induction Circuit Concentration Depends on Architecture, Not Scale

We run a second experiment on random repeated-token sequences to test whether the IOI concentration pattern holds on a task with no semantic content. We measure ICL loss and score each head by its contribution to in-context prediction. Table 3 shows results across both families.

Pythia-1.4B and 6.9B both solve the task but require 22 and 28 ablations respectively. The Pythia induction circuit becomes more distributed as scale increases, not less. Within Qwen2.5, all three models break in two to six ablations across a 14× parameter range. Qwen2.5-7B at 7B parameters needs 6 ablations while Pythia-1.4B at 1.4B needs 22. The concentration advantage of GQA holds even when comparing a model five times larger against a smaller MHA baseline. Figure 3 shows the ablation curves for both families.

Table 1. IOI results across Pythia (MHA) and Qwen2.5 (GQA). Baseline logit diff measures model confidence in the correct recipient. Top head score is the logit diff drop from ablating the single most important head.

Model	Baseline Logit Diff	Top Head Score	Top Head Layer	Heads-to-80%
Pythia-160M	0.290	0.108	L8	5
Pythia-1.4B	0.408	0.231	L12	2
Pythia-6.9B	0.546	0.250	L16	3
Qwen2.5-0.5B	0.389	0.772	L23	1
Qwen2.5-1.5B	1.368	1.860	L0	1
Qwen2.5-7B	0.791	0.948	L0	1

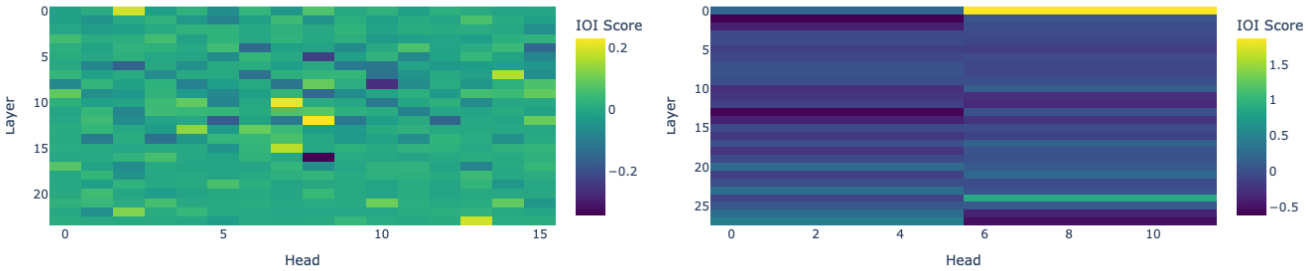

Figure 1. IOI head contribution score heatmaps for Pythia-1.4B (left) and Qwen2.5-1.5B (right) at matched scales. Each cell is the logit diff drop when that (layer, head) pair is ablated. Pythia-1.4B shows diffuse contributions spread across many layers and heads. Qwen2.5-1.5B shows a single bright band at layer 0, a direct consequence of GQA sharing KV heads across all query heads in that layer.

Table 3. Induction head results on random repeated-token sequences. ICL advantage is random-chance loss minus baseline loss. Pythia-160M has negative ICL advantage and no measurable induction circuit. Ablating up to 20 heads causes no meaningful damage, so its Heads-to-80% entry exceeds 20.

Model	ICL Adv	Top Head Score	Heads-to-80%
Pythia-160M	−7.668	0.672	>20
Pythia-1.4B	+5.845	0.877	22
Pythia-6.9B	+5.565	0.766	28
Qwen2.5-0.5B	+6.456	0.912	2
Qwen2.5-1.5B	+7.388	0.965	6
Qwen2.5-7B	+6.278	0.869	6

5.3. Factual Recall Undergoes a Phase Transition in GQA Models

Table 4 shows factual recall results across both families and both analysis conditions.

Pythia factual recall circuits are markedly diffuse. The shared fact analysis requires 50 to 135 ablations to cause 80% accuracy damage. All three models show peak factual signal only in the final layers (Meng et al., 2022). Pythia-1.4B and Pythia-6.9B show substantially different top heads and critical layers between per-model and shared fact conditions. On shared (easier) facts, no single layer causes more than 30% damage. On harder per-model facts, the circuit concentrates in mid-to-late layers and layer 16 causes 100% damage for Pythia-6.9B. This does not appear in Qwen2.5, which shows identical top heads and layer profiles across both conditions.

All three Qwen2.5 models require exactly one ablation to cause 80% accuracy damage on both per-model and shared facts. A discrete phase transition occurs between 0.5B and 1.5B. Qwen2.5-0.5B concentrates factual recall at layer 4 and requires eight ablations to break. Qwen2.5-1.5B and 7B concentrate entirely at layer 0 and break with a single ablation. Figure 4 shows this directly: ablating all heads in layer 0 collapses accuracy to zero for Qwen2.5-1.5B and 7B while causing only moderate damage for Qwen2.5-0.5B. The profile is identical between per-model and shared fact conditions, showing that the Qwen2.5 circuit location is stable across fact difficulty.

Table 5 shows how the bottleneck breaks down at the KV head level: ablating the single top KV head at layer 0 causes 97.2% accuracy damage for Qwen2.5-1.5B and 92.8% for Qwen2.5-7B, while the same ablation causes only 36.4% damage for Qwen2.5-0.5B.

Table 5. Layer 0 ablation diagnostic for Qwen2.5 factual recall. Acc. after L0 ablation is the remaining accuracy after ablating all attention heads in layer 0. Drop (%) is the accuracy reduction when all attention heads at layer 0 are ablated simultaneously.

Model	Top Head	Acc. after L0 Ablation	Drop (%)
Qwen2.5-0.5B	L4 H7	0.345	36.4
Qwen2.5-1.5B	L0 H6	0.017	97.2
Qwen2.5-7B	L0 H0	0.048	92.8

For Qwen2.5-1.5B, ablating KV head 1 at layer 0 alone collapses accuracy to 0.017, while control ablations at any

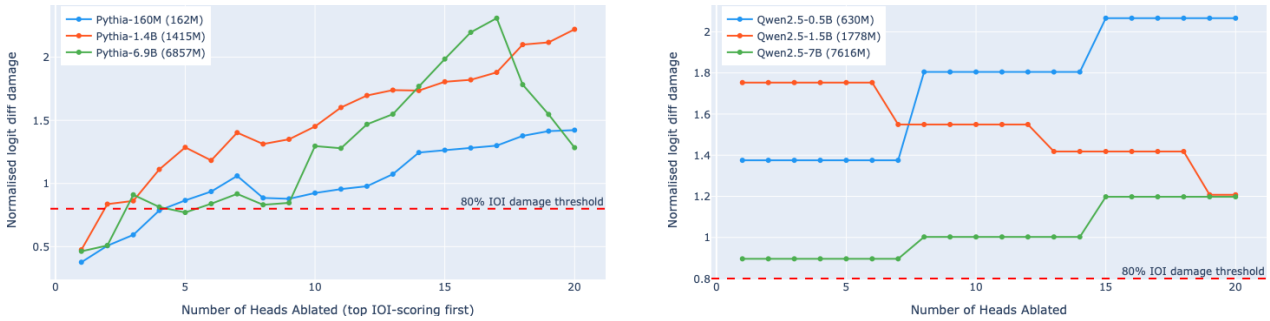

Figure 2. IOI ablation curves for Pythia (left) and Qwen2.5 (right). The y-axis is normalised logit diff damage. The x-axis is heads ablated in greedy order. Pythia models require multiple ablations before crossing the 80% threshold. All three Qwen2.5 models exceed 80% damage after the first ablation and remain there which confirms that a single head carries the circuit.

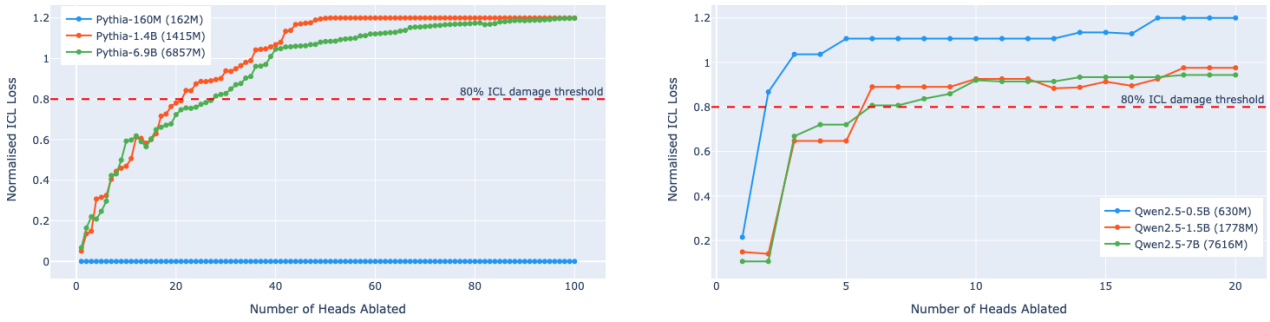

Figure 3. ICL ablation curves for Pythia (left) and Qwen2.5 (right). Pythia-160M flatlines at zero, showing no functional induction heads. Pythia-1.4B and 6.9B rise gradually and cross the threshold only after many ablations. Qwen2.5 models cross 80% within the first few ablations and plateau, showing the circuit is carried by very few heads regardless of scale.

other layer improve accuracy. Qwen2.5-7B shows the same structure. Qwen2.5-0.5B shows a different structure: the top head is at layer 4 head 7 and ablating both layer 0 and layer 4 together leaves 12.7% residual accuracy, pointing to a partial backup pathway. This dual bottleneck places 0.5B below the phase transition threshold. On shared facts, no single layer causes more than 30% accuracy damage for Pythia-1.4B or Pythia-6.9B, showing that MHA models have no comparable bottleneck structure.

Across all three circuit types, Qwen2.5 GQA models require one to six ablations to cause 80% circuit damage while Pythia MHA models require 4 to 135. At matched scales, Pythia-1.4B versus Qwen2.5-1.5B, the difference is 50 versus 1 ablation for shared factual recall and 22 versus 6 for induction heads. Architecture drives this difference.

6. Implications

Architecture is a first-class variable for mechanistic interpretability. GQA versus MHA predicts circuit concentration more reliably than parameter count. Most deployed frontier models already use GQA or similar KV-sharing mechanisms for inference efficiency. Large deployed models may therefore be substantially more amenable to circuit-level analysis than is commonly assumed. Interpretability tool development should benchmark across architecture families rather than model sizes alone. These results are encouraging for interpretability-based safety monitoring. GQA circuits are stable across fact difficulty while MHA circuits shift substantially between input regimes. A monitoring tool built on a GQA circuit will behave consistently across inputs while a tool built on an MHA circuit may not. Identifying circuits is necessary but not sufficient for reliable oversight. Circuits must also be verified to remain stable under deployment conditions.

7. Limitations

Our fact set covers world geography, science, history, and culture. The factual recall findings may not generalise to facts requiring multi-hop reasoning or temporal context. We cannot fully separate architecture from training. Pythia and Qwen2.5 differ in training data, tokenizer, and training recipe in addition to attention mechanism. The GQA hypothesis is the most parsimonious explanation but a controlled experiment with matched models trained with and without GQA would be needed to isolate the architectural effect. Our study covers three circuit types chosen for their prior literature support. Whether the architecture-driven concentration pattern holds for circuits underlying safety-relevant behaviours such as deception or goal-directed reasoning

Table 4. Factual recall results across Pythia and Qwen2.5 under per-model and shared fact conditions. H-80% is the number of heads ablated to cause 80% accuracy damage. Qwen2.5 circuit geometry is identical across both conditions at every scale. Pythia circuit geometry shifts substantially between per-model and shared facts, reflecting sensitivity to fact difficulty.

Model	Facts (per)	Facts (shared)	Heads-to-80% (per)	Heads-to-80% (shared)
Pythia-160M	91	84	135	135
Pythia-1.4B	265	84	36	50
Pythia-6.9B	357	84	4	93
Qwen2.5-0.5B	267	230	1	1
Qwen2.5-1.5B	299	230	1	1
Qwen2.5-7B	330	230	1	1

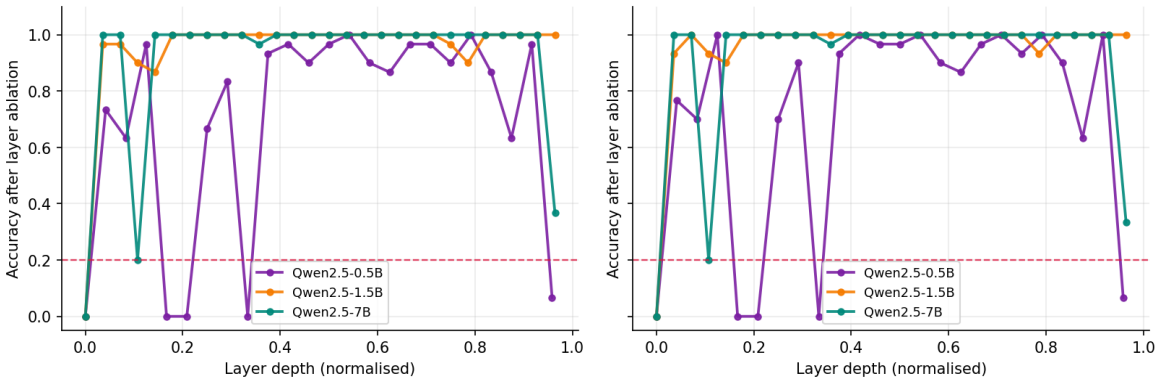

Figure 4. Layer-wise ablation for Qwen2.5 factual recall. Each point shows accuracy after ablating all heads in that layer. Per-model facts (left) and shared facts (right) show identical profiles, showing the circuit location is stable across input conditions.

remains an open question.

8. Conclusion

Mechanistic interpretability difficulty is not a monotone function of model size. Across three circuit types and six models, we find that the attention mechanism determines circuit geometry more reliably than parameter count. GQA models produce circuits that concentrate into one or two heads, remain stable across input conditions, and break cleanly under targeted ablation. MHA models at comparable scales produce circuits that are diffuse, input-sensitive, and resistant to surgical intervention. GQA was designed for inference efficiency. Its effect on circuit tractability is a consequence of structural constraints on value-space computation, not an intended property. This architectural choice incidentally produces more interpretable models at scale. The field should take this into account when deciding which models to prioritise for study and which design choices to encourage.

Acknowledgements

We thank the mechanistic interpretability community for open-sourcing TransformerLens. Experiments were conducted using publicly available models from Hugging Face. We also thank RunPod for providing compute resources.

Impact Statement

This work studies how attention architecture affects mechanistic interpretability. GQA, already widely adopted for inference efficiency, incidentally produces more tractable circuits at scale. We hope this encourages interpretability research on deployed models and evaluation of tools across architecture families. More broadly, a better understanding of what makes models interpretable at the architectural level may inform safer model design choices and support the development of reliable oversight tools for deployed AI systems. All model weights, datasets and libraries used in this work are publicly available and were used in accordance with their respective licenses and terms of use.

References

Ainslie, J., Lee-Thorp, J., De Jong, M., Zemlyanskiy, Y., Lebrón, F., and Sanghai, S. Gqa: Training generalized multi-query transformer models from multi-head checkpoints. In *Proceedings of the 2023 Conference on Empirical Methods in Natural Language Processing*, pp. 4895–4901, 2023.

Biderman, S., Schoelkopf, H., Anthony, Q. G., Bradley, H., O'Brien, K., Hallahan, E., Khan, M. A., Purohit, S., Prashanth, U. S., Raff, E., et al. Pythia: A suite for analyzing large language models across training and

scaling. In *International conference on machine learning*, pp. 2397–2430. PMLR, 2023.

Conmy, A., Mavor-Parker, A., Lynch, A., Heimersheim, S., and Garriga-Alonso, A. Towards automated circuit discovery for mechanistic interpretability. *Advances in Neural Information Processing Systems*, 36:16318–16352, 2023.

Cordonnier, J.-B., Loukas, A., and Jaggi, M. Multi-head attention: Collaborate instead of concatenate. *arXiv preprint arXiv:2006.16362*, 2020.

Elhage, N., Nanda, N., Olsson, C., Henighan, T., Joseph, N., Mann, B., Askell, A., Bai, Y., Chen, A., Conerly, T., et al. A mathematical framework for transformer circuits. *Transformer Circuits Thread*, 1(1):12, 2021.

Elhage, N., Hume, T., Olsson, C., Schiefer, N., Henighan, T., Kravec, S., Hatfield-Dodds, Z., Lasenby, R., Drain, D., Chen, C., et al. Toy models of superposition. *arXiv preprint arXiv:2209.10652*, 2022.

Fahamu. fahamu/ioi: Indirect object identification dataset. https://huggingface.co/datasets/fahamu/ioi, 2023.

Ganguli, D., Lovitt, L., Kernion, J., Askell, A., Bai, Y., Kadavath, S., Mann, B., Perez, E., Schiefer, N., Ndousse, K., et al. Red teaming language models to reduce harms: Methods, scaling behaviors, and lessons learned. *arXiv preprint arXiv:2209.07858*, 2022.

Geva, M., Schuster, R., Berant, J., and Levy, O. Transformer feed-forward layers are key-value memories. In *Proceedings of the 2021 Conference on Empirical Methods in Natural Language Processing*, pp. 5484–5495, 2021.

Geva, M., Bastings, J., Filippova, K., and Globerson, A. Dissecting recall of factual associations in auto-regressive language models. In *Proceedings of the 2023 Conference on Empirical Methods in Natural Language Processing*, pp. 12216–12235, 2023.

Hernandez, E., Sharma, A. S., Haklay, T., Meng, K., Wattenberg, M., Andreas, J., Belinkov, Y., and Bau, D. Linearity of relation decoding in transformer language models. *arXiv preprint arXiv:2308.09124*, 2023.

Lieberum, T., Rahtz, M., Kramár, J., Nanda, N., Irving, G., Shah, R., and Mikulik, V. Does circuit analysis interpretability scale? evidence from multiple choice capabilities in chinchilla. *arXiv preprint arXiv:2307.09458*, 2023.

Lindsey, J., Gurnee, W., Ameisen, E., Chen, B., Pearce, A., Turner, N. L., Citro, C., Abrahams, D., Carter, S., Hosmer, B., Marcus, J., Sklar, M., Templeton, A., Bricken, T., McDougall, C., Cunningham, H., Henighan, T., Jermyn, A., Jones, A., Persic, A., Qi, Z., Thompson, T. B., Zimmerman, S., Rivoire, K., Conerly, T., Olah, C., and Batson, J. On the biology of a large language model. *Transformer Circuits Thread*, 2025. URL https://transformer-circuits.pub/2025/attribution-graphs/biology.html.

Marks, S. and Tegmark, M. The geometry of truth: Emergent linear structure in large language model representations of true/false datasets. *arXiv preprint arXiv:2310.06824*, 2023.

McDougall, C. S., Conmy, A., Rushing, C., McGrath, T., and Nanda, N. Copy suppression: Comprehensively understanding a motif in language model attention heads. In *Proceedings of the 7th BlackboxNLP Workshop: Analyzing and Interpreting Neural Networks for NLP*, pp. 337–363, 2024.

Meng, K., Bau, D., Andonian, A., and Belinkov, Y. Locating and editing factual associations in gpt. *Advances in neural information processing systems*, 35:17359–17372, 2022.

Nanda, N. and Bloom, J. Transformerlens. https://github.com/TransformerLensOrg/TransformerLens, 2022.

Olah, C., Cammarata, N., Schubert, L., Goh, G., Petrov, M., and Carter, S. Zoom in: An introduction to circuits. *Distill*, 5(3):e00024–001, 2020.

Olsson, C., Elhage, N., Nanda, N., Joseph, N., DasSarma, N., Henighan, T., Mann, B., Askell, A., Bai, Y., Chen, A., et al. In-context learning and induction heads. *arXiv preprint arXiv:2209.11895*, 2022.

Templeton, A. *Scaling monosemanticity: Extracting interpretable features from claude 3 sonnet*. Anthropic, 2024.

Wang, K., Variengien, A., Conmy, A., Shlegeris, B., and Steinhardt, J. Interpretability in the wild: a circuit for indirect object identification in gpt-2 small. *arXiv preprint arXiv:2211.00593*, 2022.

Yang, A., Yang, B., Zhang, B., Hui, B., Zheng, B., Yu, B., Li, C., Liu, D., Huang, F., Wei, H., et al. Qwen2.5 technical report. *arXiv preprint arXiv:2412.15115*, 2024.

A. Factual Recall Dataset: Domain Coverage and Prompt Format

Table 6. Five sample prompts per domain from the 493-fact set. Answers are single tokens.

Domain	Sample Prompts (answer)
World Geography	The capital of France is (*Paris*) The Nile River is located in (*Egypt*) The Eiffel Tower is located in (*Paris*) The largest ocean in the world is the (*Pacific*) The largest country by area is (*Russia*)
Science & Chemistry	The chemical symbol for gold is (*Au*) The largest organ in the human body is the (*skin*) The atomic number of hydrogen is (*1*) The SI unit of length is (*meter*) The hardest natural material is (*diamond*)
History	World War II ended in (*1945*) The French Revolution began in (*1789*) The Berlin Wall fell in (*1989*) The first moon landing occurred in (*1969*) India gained independence in (*1947*)
Notable People	Marie Curie was born in (*Poland*) Isaac Newton was born in (*England*) Aristotle was a student of (*Plato*) Albert Einstein was born in (*Germany*) Mahatma Gandhi was born in (*India*)
Literature & Arts	The author of 1984 is (*George*) The Mona Lisa was painted by (*Leonardo*) The Starry Night was painted by (*Vincent*) Swan Lake was composed by (*Tchaikovsky*) The author of Hamlet is (*William*)
Technology	Apple was founded by (*Steve*) Linux was created by (*Linus*) The iPhone was first released in (*2007*) Python was created by (*Guido*) Google was founded by (*Larry*)
Sports	The FIFA World Cup is held every (*four*) years Basketball was invented by (*James*) Golf originated in (*Scotland*) Cricket originated in (*England*) Wimbledon is held in (*London*)
Food & Culture	Pizza originated in (*Italy*) Sushi originated in (*Japan*) Coffee originated in (*Ethiopia*) Vodka originated in (*Russia*) Champagne is produced in (*France*)
Mythology & Religion	The king of Greek gods is (*Zeus*) The Norse god of thunder is (*Thor*) The sacred text of Islam is the (*Quran*) Islam was founded by (*Muhammad*) The holy city of Islam is (*Mecca*)
Currencies & Languages	The currency of Japan is the (*yen*) The currency of India is the (*rupee*) The official language of China is (*Mandarin*) The official language of Brazil is (*Portuguese*) The most spoken language is (*Mandarin*)

Table 6 shows five representative prompts from each domain in the 493-fact set. All prompts follow a natural cloze completion format and require single-token answers. The fact set spans ten domains chosen to ensure diverse coverage of world knowledge while avoiding multi-hop reasoning or temporal context.

B. Additional Results

B.1. Top Contributing IOI Heads per Model

Table 7 shows the top-5 IOI contributing heads for each model. For Qwen2.5-1.5B all five top heads are at layer 0 and for Qwen2.5-7B all five are also at layer 0. The GQA row structure is visible directly: because KV heads are shared across query heads, ablating one KV head ablates an entire row of query heads simultaneously, concentrating the damage at the shared layer. For Pythia, the top-5 heads are distributed across multiple layers with no dominant layer. Across all six models, the top-scoring IOI head and the top-scoring ICL head are different individual heads, yet the circuit concentration pattern is consistent within each architecture family across both tasks. The architecture-driven concentration effect is a property of how the architecture organises computation, not of any single head.

Table 7. Top-5 IOI contributing heads per model by (layer, head) index.

Model	Top-5 heads (layer, head)
Pythia-160M	(8,9), (7,11), (3,3), (1,6), (11,3)
Pythia-1.4B	(12,8), (10,7), (0,2), (23,13), (15,7)
Pythia-6.9B	(16,30), (24,26), (27,30), (25,24), (23,18)
Qwen2.5-0.5B	(23,0), (23,1), (23,2), (23,3), (23,4)
Qwen2.5-1.5B	(0,6), (0,7), (0,8), (0,9), (0,10)
Qwen2.5-7B	(0,1), (0,2), (0,3), (0,4), (0,5)

B.2. Pythia Fact-Difficulty Diagnostic

Table 8 reports the top-scoring head and mean logit gap for Pythia-6.9B and Pythia-1.4B under per-model and shared fact conditions. The top head changes substantially between conditions for both models and the logit gap is higher on shared (easier) facts for both. This supports the fact-difficulty dependent circuit geometry claim in the main results.

Table 8. Pythia diagnostic results comparing per-model and shared fact conditions. Top head layer shows where the primary contributing head is located under each condition.

Model	Condition	Logit Gap	Top Head Layer	Top Head Score
Pythia-1.4B	Per-model	1.006	L12	0.903
	Shared	1.202	L23	0.552
Pythia-6.9B	Per-model	0.647	L4	0.655
	Shared	1.098	L16	0.827

B.3. IOI Head Contribution Score Heatmaps

Figure 5 shows IOI head contribution score heatmaps for all six models. The architecture contrast is visible at every scale: Pythia heatmaps show diffuse scattered contributions while Qwen2.5 heatmaps show a single concentrated band.

B.4. ICL Induction Head Score Heatmaps

Figure 6 shows ICL induction head score heatmaps for all six models on the secondary random repeated-token task. The same architecture contrast holds: Pythia heatmaps show scattered induction scores across the full layer-head matrix while Qwen2.5 heatmaps show a smaller number of dominant heads.

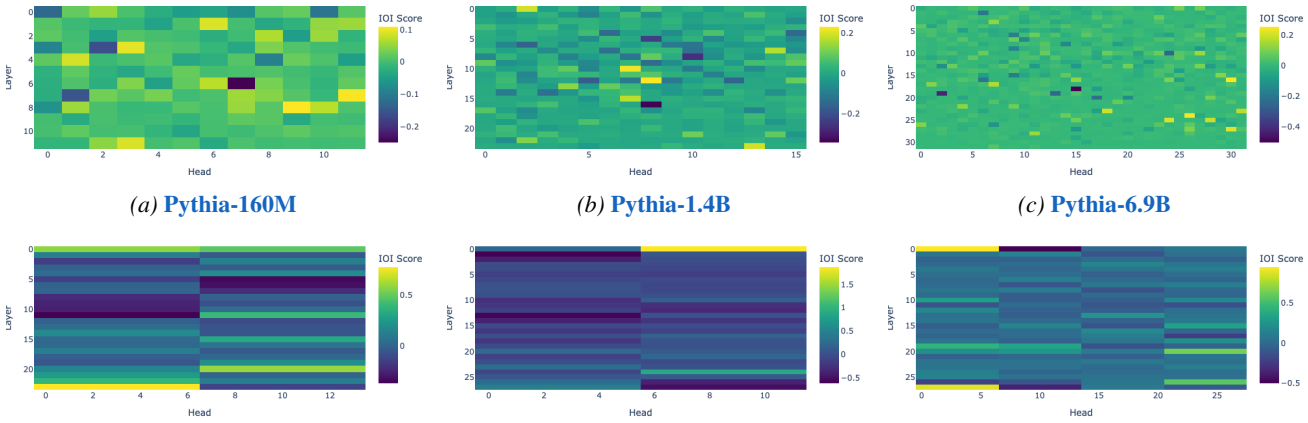

(a) **Pythia-160M** *(b)* **Pythia-1.4B** *(c)* **Pythia-6.9B**

(d) **Qwen2.5-0.5B** *(e)* **Qwen2.5-1.5B** *(f)* **Qwen2.5-7B**

Figure 5. IOI head contribution score heatmaps across all six models. Each cell shows the logit diff drop when that (layer, head) pair is ablated. **Pythia (MHA)** shows contributions scattered across many layers and heads with no dominant structure. **Qwen2.5 (GQA)** shows a single bright band at layer 0 for 1.5B and 7B and at layer 23 for 0.5B, reflecting the phase transition between these scales.

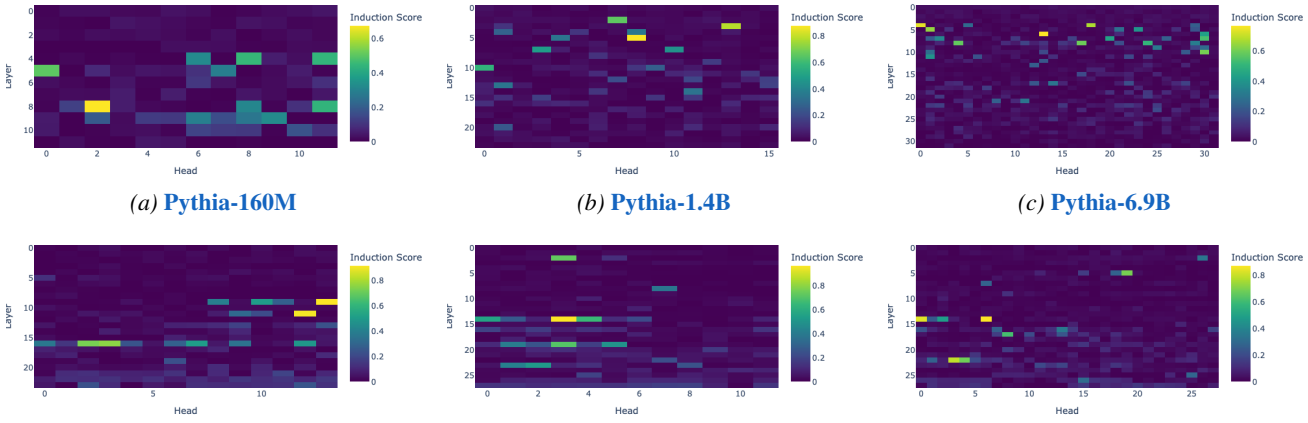

(a) **Pythia-160M** *(b)* **Pythia-1.4B** *(c)* **Pythia-6.9B**

(d) **Qwen2.5-0.5B** *(e)* **Qwen2.5-1.5B** *(f)* **Qwen2.5-7B**

Figure 6. ICL induction head score heatmaps across all six models on random repeated-token sequences. Each cell shows the mean attention weight at the induction offset position for that (layer, head) pair. **Pythia (MHA)** shows induction scores scattered across the full layer-head matrix. Pythia-160M has one dominant cell at layer 8 but Pythia-1.4B and 6.9B show increasing scatter with no clearly dominant layer and the number of high-scoring heads grows with scale. **Qwen2.5 (GQA)** shows induction scores concentrated in specific mid-to-late layer bands. Qwen2.5-1.5B shows a bright cluster around layers 14-20 with fewer active heads. Qwen2.5-7B shows a similar mid-network concentration, with notably fewer high-scoring cells than Pythia-6.9B at comparable scale.